

## 1 Charmless $B$ Decay Measurements at Belle II

---

2 **Sagar Hazra**

3 *Tata Institute of Fundamental Research,*  
4 *Mumbai 400 005, India*

5 *E-mail: [sagar.hazra@tifr.res.in](mailto:sagar.hazra@tifr.res.in)*

6 We report the measurements of  $CP$  asymmetry and branching fraction of various charmless  $B$  decays performed using  $e^+e^-$  collision data recorded at the  $\Upsilon(4S)$  resonance with the Belle II detector at the SuperKEKB collider. These include a test of the standard model using isospin sum rule, an investigation of localized  $CP$  asymmetries in the Dalitz plot, and an expected improvement on the precision of the CKM unitarity angle  $\phi_2/\alpha$ . All the results agree with the previous determinations and contribute important information to an early assessment of Belle II performance.

*11th International Workshop on the CKM Unitarity Triangle (CKM2021)*  
*November 22–26, 2021*  
*The University of Melbourne, Australia*

## 1. Introduction

The study of charmless  $B$  decays is a keystone of the worldwide flavor physics program to test the standard model (SM) and its extension. These decays mediated by Cabibbo-suppressed  $b \rightarrow u$  tree and  $b \rightarrow d, s$  loop transitions are sensitive to non-SM contributions. They also provide the access to the three CKM unitarity angles. Furthermore, we can test the prediction of an isospin sum rule [1], given by

$$\mathcal{A}_{+c^-} + \mathcal{A}_{0c^+} \frac{\mathcal{B}(K^0\pi^+) \tau_0}{\mathcal{B}(K^+\pi^-) \tau_+} - 2\mathcal{A}_{+c^0} \frac{\mathcal{B}(K^+\pi^0) \tau_0}{\mathcal{B}(K^+\pi^-) \tau_+} - 2\mathcal{A}_{0c^0} \frac{\mathcal{B}(K^0\pi^0)}{\mathcal{B}(K^+\pi^-)} = 0, \quad (1)$$

that combines the branching fraction ( $\mathcal{B}$ ) and direct  $CP$  asymmetry ( $\mathcal{A}_{\%}$ ) values measured in  $B$  decays to four possible  $K\pi$  final states:  $K^+\pi^-$ ,  $K^0\pi^+$ ,  $K^+\pi^0$ , and  $K^0\pi^0$ . Belle II has a unique capability of studying jointly, and within a consistent experimental environment for, all the relevant final states towards a consistency test of the SM.

## 2. The Belle II detector

Belle II [2] is a magnetic spectrometer having almost  $4\pi$  solid-angle coverage, designed to reconstruct final-state particles of  $e^+e^-$  collisions delivered by the SuperKEKB asymmetric-energy collider [3], located at the KEK laboratory in Tsukuba, Japan. The energies of the positron and electron beams are 4 and 7 GeV, respectively. Belle II comprises a number of subdetectors surrounding the interaction point (IP) in a cylindrical geometry. The innermost one is the vertex detector, which uses position-sensitive silicon layers to sample the trajectories of charged particles ('tracks') in the vicinity of the IP to determine the decay positions of their long-lived parent particles. Charged-particle momenta and charges are measured by a large-radius, helium-ethane, small-cell drift chamber, which also offers charged-particle-identification information via a measurement of specific ionization. A Cherenkov-light angle and time-of-propagation detector surrounding the drift chamber provides charged-particle identification in the central detector volume, supplemented by proximity-focusing, aerogel, ring-imaging Cherenkov detector in the forward region with respect to the electron beam. A CsI(Tl)-crystal electromagnetic calorimeter provides electron-energy measurements and photon reconstruction. Layers of plastic scintillators and resistive-plate chambers, interspersed between the magnetic flux-return iron plates, allow for the identification of  $K_L^0$  and muons.

## 3. Analysis overview

We form final-state particle candidate by applying loose baseline selection criteria and then combine them in kinematic fits consistent with the topologies of the desired decays to reconstruct intermediate states and  $B$  candidates. We then apply optimized continuum suppression and particle identification criteria. Signal reconstruction efficiencies are calculated from simulation and validated on data themselves. For the signal extraction, we develop fit model from simulation, later adjusted according to high-statistics control channels. To determine the systematic uncertainties, pseudo-experiment and control channel studies are performed. For the validation purpose, we

42 perform full analysis on control channel. We then inspect the most interesting region (or, signal  
43 region) on data to measure the physics observables.

#### 44 4. Challenges

45 The key challenge in reconstructing significant charmless signal is the large contamination from  
46  $e^+e^- \rightarrow q\bar{q}$  ( $q = u, d, s, c$ ) continuum background coupled with low signal branching fraction.  
47 We use a binary-decision-tree classifier that combines a number of mostly topological variables  
48 having some discrimination between  $B$ -meson signal and continuum background. We pick up those  
49 variables whose correlation with  $E$  and  $M_{bc}$  is below  $\pm 5\%$  to reduce possible bias in the signal  
50 yield determination. The latter two are the energy difference  $E = E^* - \sqrt{s}/2$  between the energy  
51 of the reconstructed  $B$  candidate and half of the collision energy, both in the  $\Upsilon(4S)$  frame, and the  
52 beam-energy-constrained mass  $M_{bc} = \sqrt{s/(4c^4) - (p^*/c)^2}$ , which is the invariant mass of the  $B$   
53 candidate with its energy being replaced by the half of the center-of-mass collision energy. Another  
54 challenge is to separate  $B$  background events that peak in the signal region. To deal with this peaking  
55 background, we either kinematically veto it from the sample or include a separate component in  
56 the fit model. For example, the background from  $B^+ \rightarrow \bar{D}^0(\rightarrow K^+\pi^-)\pi^+$  decays is suppressed by  
57 vetoing candidates with a kaon-pion mass in the range  $[1.84, 1.89] \text{ GeV}/c^2$ .

#### 58 5. Results

##### 59 5.1 Isospin sum-rule

60 The isospin sum-rule relation for the  $B \rightarrow K\pi$  system given in Eq. (1) provides a stringent  
61 test of the SM. In all the four  $K\pi$  channels, signal yields are determined with unbinned extended  
62 maximum-likelihood fits of the  $E$  and  $M_{bc}$  distributions. The  $B^0 \rightarrow K^0\pi^0$  channel is most  
63 challenging one as it requires the reconstruction of two neutral particles, namely  $K^0$  and  $\pi^0$ . We  
64 measure the time-integrated asymmetry of the  $CP$ -eigenstate  $B^0 \rightarrow K^0\pi^0$  with the signal-side quark  
65 flavor  $q$  obtained using the flavor content of the other  $B$ -meson, provided by the category-based  
66 flavor tagger [4]. The asymmetry  $\mathcal{A}_{0c^0}$  is determined from a simultaneous maximum-likelihood  
67 fit to the unbinned  $M_{bc}-E-q$  distributions. The signal probability density function (PDF) is given  
68 by

$$\mathcal{P}_{\text{sig}} = \frac{1}{2} [1 + q(1 - 2w_A) \cdot (1 - 2\chi_3)\mathcal{A}_{0c^0}], \quad (2)$$

69 where  $\chi_3$  is the  $B^0-\bar{B}^0$  mixing frequency,  $w_A$  is the wrong tag fraction in each dilution ( $r$ ) interval.  
70 Figures 1 and 2 show the  $E$  distribution of all the four  $K\pi$  system. We obtain the following  
71 branching fractions,

$$\begin{aligned} \mathcal{B}(B^0 \rightarrow K^+\pi^-) &= [18.0 \pm 0.9(\text{stat}) \pm 0.9(\text{syst})] \times 10^{-6}, \\ \mathcal{B}(B^+ \rightarrow K^+\pi^0) &= [11.9_{-1.0}^{+1.1}(\text{stat}) \pm 1.6(\text{syst})] \times 10^{-6}, \\ \mathcal{B}(B^+ \rightarrow K^0\pi^+) &= [21.4_{-2.2}^{+2.3}(\text{stat}) \pm 1.6(\text{syst})] \times 10^{-6}, \\ \mathcal{B}(B^0 \rightarrow K^0\pi^0) &= [8.5_{-1.6}^{+1.7}(\text{stat}) \pm 1.2(\text{syst})] \times 10^{-6} \end{aligned}$$



81 and  $CP$ -violating rate asymmetries

$$\begin{aligned}\mathcal{A}_{\%}(B^+ \rightarrow K^+ K^- K^+) &= -0.103 \pm 0.042(\text{stat}) \pm 0.020(\text{syst}), \\ \mathcal{A}_{\%}(B^+ \rightarrow K^+ \pi^- \pi^+) &= -0.010 \pm 0.050(\text{stat}) \pm 0.021(\text{syst}), \\ \mathcal{A}_{\%}(B^0 \rightarrow K^+ \pi^- \pi^0) &= +0.207 \pm 0.088(\text{stat}) \pm 0.011(\text{syst}).\end{aligned}$$

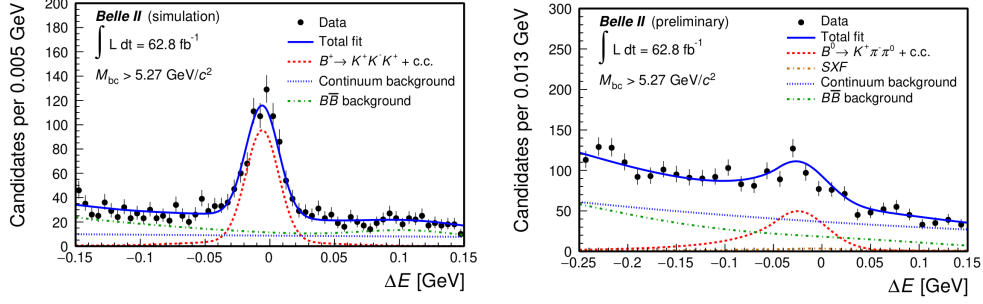


Figure 3: Signal-enhanced  $E$  distributions of  $B^+ \rightarrow K^+ K^- K^+$  (left) and  $B^0 \rightarrow K^+ \pi^- \pi^0$  (right).

82

### 83 5.1.2 Determination of $\alpha/\phi_2$

84 The study of charmless decays at Belle II can provide improved measurements of the CKM  
85 unitarity angle  $\alpha/\phi_2 = \arg -\frac{+c_3 + 2_1}{+D_3 + D_1}$ , where  $V_{ij}$  are elements of the quark-mixing matrix. In par-  
86 ticular, the combined analysis of branching fractions and  $CP$  violating asymmetries of the complete  
87 set of  $B \rightarrow \pi\pi, \rho\rho$  isospin partners enables a determination of  $\alpha$  [5]. The  $B^0 \rightarrow \pi^0\pi^0$  channel is  
88 particularly challenging as it requires two  $\pi^0$  reconstruction. A dedicated boosted decision-trees  
89 classifier used to suppress background photons by combining 20 calorimetric variables. Signal  
90 yields are determined with an extended maximum-likelihood fit of the  $E$ ,  $M_{bc}$  and transformed  
91 continuum suppression variable. Figure 4 shows the  $E$  distribution of two  $\pi\pi$  channels. We obtain  
92 the following branching fractions,

$$\begin{aligned}\mathcal{B}(B^0 \rightarrow \pi^+ \pi^-) &= [5.8 \pm 0.7(\text{stat}) \pm 0.7(\text{syst})] \times 10^{-6}, \\ \mathcal{B}(B^+ \rightarrow \pi^+ \pi^0) &= [5.5_{-0.9}^{+1.0}(\text{stat}) \pm 0.7(\text{syst})] \times 10^{-6}, \\ \mathcal{B}(B^0 \rightarrow \pi^0 \pi^0) &= [0.98_{-0.39}^{+0.48}(\text{stat}) \pm 0.27(\text{syst})] \times 10^{-6}\end{aligned}$$

93 and  $CP$  asymmetry of  $\mathcal{A}_{\%}(B^+ \rightarrow \pi^+ \pi^0) = -0.04 \pm 0.17(\text{stat}) \pm 0.06(\text{syst})$ . The  $B^+ \rightarrow \rho^+ \rho^0$   
94 decay involves pion-only final state, where the large width of the  $\rho$  mesons offers reduced distinctive  
95 features against dominant continuum background. Isolating a low-background signal is therefore the  
96 main challenge of the analysis. Signal yields are determined with an unbinned maximum-likelihood  
97 fits of  $E$ , continuum-suppression decision-tree output, the dipion masses and cosines of helicity  
98 angles of the  $\rho$  candidates. Figure 5 shows the  $E$  and log transform continuum-suppression output  
99 of  $B^+ \rightarrow \rho^+ \rho^0$  candidates. We obtain the branching fraction  $\mathcal{B} = [20.6 \pm 3.2(\text{stat}) \pm 4.0(\text{syst})] \times 10^{-6}$   
100 and longitudinal polarization fraction  $f_l = 0.936_{-0.041}^{+0.049}(\text{stat}) \pm 0.021(\text{syst})$ .

